

# Vegetation and Evapotranspiration Responses to Increased Atmospheric Vapor Pressure Deficit across the Global Forest

Rihong Wen <sup>1,2,†</sup>, Meiou Qin <sup>3,†</sup>, Peng Jiang <sup>1,2,4,\*</sup>, Feiyun Yang <sup>5</sup>, Bin Liu <sup>4</sup>, Mengyuan Zhu <sup>6</sup>, Yuan Fang <sup>1,4</sup>, Yichen Tian <sup>1,4</sup> and Bo Shang <sup>7,\*</sup>

<sup>1</sup> Institute of Atmospheric Environment, China Meteorological Administration, Shenyang 110166, China; fangyuan@iaesy.cn (Y.F.)

<sup>2</sup> Panjin National Climate Observatory, Panjin 124000, China

<sup>3</sup> Regional Climate Center of Shenyang, Shenyang 110166, China

<sup>4</sup> Liaoning Ecological Meteorology and Satellite Remote Sensing Center, Shenyang 110166, China

<sup>5</sup> China Meteorological Administration Training Center, Beijing 100081, China

<sup>6</sup> College of Agronomy, Shenyang Agricultural University, Shenyang 110161, China

<sup>7</sup> Changchun Meteorological Service, Changchun 130051, China

\* Correspondence: jiangpenglnqx@iaesy.cn (P.J.); shangbobosea@163.com (B.S.)

† These authors contributed equally to this work.

**Abstract:** A forest is vulnerable to drought and plays important roles in the regulation of carbon and water cycling in a terrestrial ecosystem. Atmospheric vapor pressure deficit (VPD) has been identified as an increasingly major factor in plant functioning and has been established as a main contributor to recent drought-induced plant mortality, independent of other drivers associated with climate change. However, most previous studies have focused on the effects of climate warming and CO<sub>2</sub> enrichment on vegetation growth, without considering the effects of an increased VPD on vegetation growth and evapotranspiration (ET) in forest ecosystems. This could lead to a large uncertainty in estimating the variability in forest carbon sinks. Based on the long-term satellite data, we investigated the response of the leaf area index (LAI) and ET to the VPD via a partial correlation analysis in this study. We also examined the temporal variability in the partial coefficients within a ten-year moving window. The results showed that over 50% of the region displayed a negative partial correlation between the LAI, ET, and VPD, and those pixels were mainly concentrated in North America and the plains of Eastern Europe. Regions with a negative trend of partial correlation in both the LAI and ET are mostly located in the plains of Eastern Europe and the Siberian Plain of western Russia, while the positive trend is mainly in South America. The plains of Eastern Europe are becoming drier, which was proved by the interannual trend of the Standardized Precipitation Evapotranspiration Index (SPEI) and soil water content (SWC). Additionally, the LAI and ET in those areas exhibited a significant positive correlation with the SWC based on the moving window average. This study suggests that the role of the VPD on vegetation will become increasingly prominent in the context of future climate change for the forest ecosystem.

**Keywords:** vapor pressure deficit; LAI; evapotranspiration; water availability; global forests



**Citation:** Wen, R.; Qin, M.; Jiang, P.; Yang, F.; Liu, B.; Zhu, M.; Fang, Y.; Tian, Y.; Shang, B. Vegetation and Evapotranspiration Responses to Increased Atmospheric Vapor Pressure Deficit across the Global Forest. *Atmosphere* **2024**, *15*, 408. <https://doi.org/10.3390/atmos15040408>

Academic Editor: Masoud Rostami

Received: 5 February 2024

Revised: 13 March 2024

Accepted: 19 March 2024

Published: 26 March 2024



**Copyright:** © 2024 by the authors. Licensee MDPI, Basel, Switzerland. This article is an open access article distributed under the terms and conditions of the Creative Commons Attribution (CC BY) license (<https://creativecommons.org/licenses/by/4.0/>).

## 1. Introduction

The terrestrial biosphere is believed to have provided a net sink for ~20% of the carbon dioxide emitted by fossil fuel burning and industry over the last three decades [1], with the majority estimated to occur in forests [2]. The growth of forests is thus believed to retard anthropogenic climate change by slowing the rate of carbon dioxide (CO<sub>2</sub>) accumulation in the atmosphere [3]. Previous studies have mainly investigated the response of forest productivity to climate warming, changes in precipitation patterns, CO<sub>2</sub> fertilization effects, and human activity. With climate change, an atmospheric VPD has been recorded in a sharp rise since the late 1990s [4] and played an important role in driving global vegetation

dynamics. However, the response of forest productivity to increasing VPD remains poorly characterized, limiting both our understanding of why it occurs and our ability to predict its continued future existence.

An increasing VPD may exert a strong impact on the carbon and water cycle in global forests. A rising VPD can significantly reduce stomatal conductance and limit the actual photosynthetic rate [5–8]. Thus, a widespread constraint of the rising VPD on global vegetation growth [4,9] or carbon sinks [10,11] has been reported in recent studies. Extended periods of high VPD have been recognized as an important determinant of large-scale tree mortality [12] and as a driver of wildfire [13]. The negative effects of an increasing VPD on vegetation growth and ET have been widely observed in forest ecosystems in water-limited regions [14]. In contrast, recent work has reported that in most of the wettest parts of subtropical and tropical forests, vegetation photosynthesis (or productivity) and ET tend to increase with a rising VPD [7,15,16]. These discrepancies suggest a large uncertainty in the impacts of an increasing VPD on the carbon and water cycle across the global forests and thus call for more investigations on this.

The carbon and water cycle responses to the increasing VPD may be regulated by soil water availability across the global forests. When the soil water availability is limited, the xylems or roots of plants sense the low water supply via an abscisic acid signal and subsequently stomatal closure in response to an increasing VPD [17]. Studies examining the dependence of the VPD impacts on soil water availability in forest ecosystems have primarily been conducted on the site scale, such as a study on a forest in south central Indiana, USA [5]. Despite that, the relationships between water availability and spatial VPD effects may be disturbed by other factors. For one, although the spatial distribution of global forests is mainly located in water-rich regions, the seasonal dryness always exerts assignable impacts on photosynthesis (or productivity) and ET [7,18,19]. Also, changes in water availability could also affect VPD effects [4], for example, the significant negative VPD effects observed in Western Europe could be due to the apparent trend toward aridification [20]. Therefore, the relationships between water availability and VPD impacts across the global forests need to be further quantified on a large spatial scale.

In sum, there is growing evidence that an increasing VPD plays an important role in driving global vegetation dynamics [4,9,11]. However, very few studies have investigated the VPD effects across global forests. Here, we used long-term satellite observations of the LAI and ET to parse the VPD impacts across the global forests. We first analyzed the spatial distribution of the response of the ET and LAI to the VPD across the global forests; subsequently, we examined whether the impacts of the VPD on ET and the LAI can be regulated by the SWC; then, we investigated the temporal changes in the VPD impacts and then analyzed the correlation of these changes with changes in the water conditions.

## 2. Materials and Methods

The Global Land Surface Satellite LAI (GLASS LAI) was used in this study. This product was generated based on Advanced Very High Resolution Radiometer (AVHRR) and Moderate Resolution Imaging Spectroradiometer (MODIS) surface reflectance data via general regression neural networks [21,22]. In particular, preprocessing should be conducted on the surface reflectance so as to mitigate the effects caused by clouds, aerosols, and sensor noise. The GLASS LAI product has been widely used in climate change, ecological environment monitoring, and other fields due to its unique features, including a long-term span (from 1982 to present), fine resolution (0.05 degree and 8-day interval), high quality, and accuracy [23,24]. The monthly actual ET and root-zone SWC data came from the Global Land Evaporation Amsterdam Model (GLEAM, v3.5a). This dataset spans over 40 years, from 1980 to 2021, at a spatial resolution of 0.25 degree [25]. The monthly air temperature ( $T_a$ ), precipitation, and actual vapor pressure (AVP) were derived from CRUST 4.04 (0.5 degree), and the monthly solar radiation (SR) was provided by the ERA5 reanalysis products (0.1 degree). Then, the VPD could be calculated according to the saturated vapor pressure (SVP) and AVP following Equations (1) and (2) [4]. The

Standardized Precipitation Evapotranspiration Index (SPEI) was used to quantify the dry/wet conditions from 1982 to 2015 and the three-month SPEI was derived from the SPEI base v2.5 at a 0.5 resolution [26,27]. For the subsequent analysis, all the data were resampled to 0.5 degrees to align to the same resolution.

$$\text{SVP} = 0.611 \times \exp\left(\frac{17.27 \times T_a}{273.3 + T_a}\right) \quad (1)$$

$$\text{VPD} = \text{SVP} - \text{AVP} \quad (2)$$

We implemented a partial correlation analysis to explore the responses of the LAI and ET to the VPD during the growing season from 1982 to 2015 after controlling the effect of the  $T_a$ , precipitation, and SR. Furthermore, we detected the temporal variability in the partial coefficients within a ten-year moving window via the Mann–Kendall test [28,29]. To access the temporal dynamics of the water availability from 1982 to 2015, we also conducted the Mann–Kendall test on the SWC and SPEI. Finally, we used the Pearson correlation analysis to estimate the relationship between the SWC and the effects of the VPD on the LAI and ET based on a ten-year moving mean value. All the statistical analyses were carried out in R (version 4.0.5) software.

### 3. Results

Overall, the negative partial correlation coefficients occupied a large proportion for both the LAI (Figure 1a) and ET (Figure 1b), with the negative partial correlations accounting for 68.6% (39.0% of pixels were significant) and 56.6% (34.9% of pixels were significant) of the total study area, respectively. The negatively correlated areas were concentrated in the Northern Hemisphere, mainly distributed in regions including North America and the plains of Eastern Europe. In contrast, the positive correlation pixels of the LAI and ET to the VPD were mainly observed in South America, Siberia, and southern China, and only a few correlations were significant.

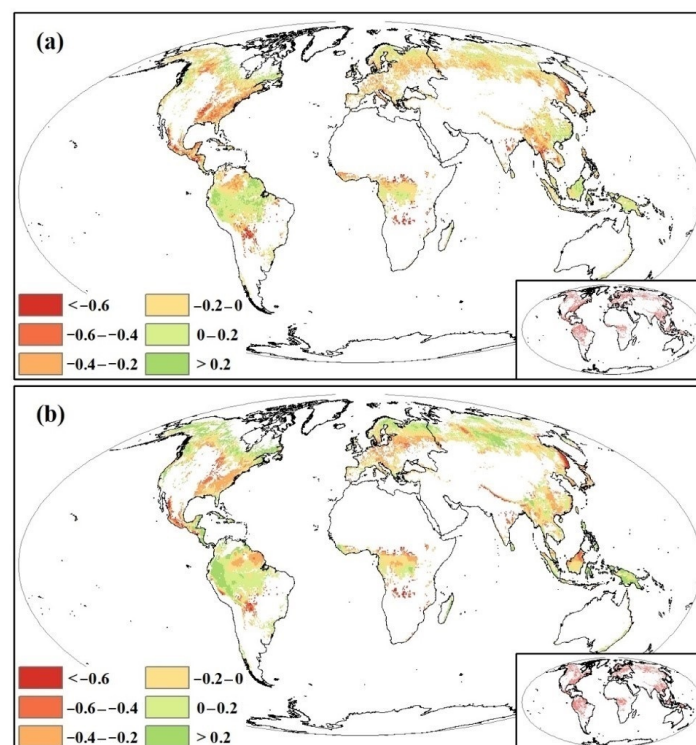


**Figure 1.** The spatial patterns of the partial correlation between LAI (a), ET (b), and VPD across the global forest ecosystem. The insets map in lower right represents the significance at the level of 0.05.

As shown in Figure 2, the proportions of the negative trend in the moving window partial correlation between the LAI and VPD were 62.1% (40.0% of the pixels were significant), and mainly distributed in the northern and eastern parts of North America, the plains of Eastern Europe, and the Siberian Plain region of western Russia. The regions that exhibited a positive trend were mainly located in South America, accounting for 53.9% of the area. As for ET, it displayed an increased trend on the whole, with 54.0% (34.4% of the pixels were significant) being positive. Similar to the LAI, the negative values were also found mainly in the northern and eastern parts of North America, the plains of Eastern Europe, and the Siberian Plain region of western Russia. Additionally, about 62.3% of the regions in Africa displayed a negative trend in ET, with 47.7% of the pixels experiencing a significant decrease.

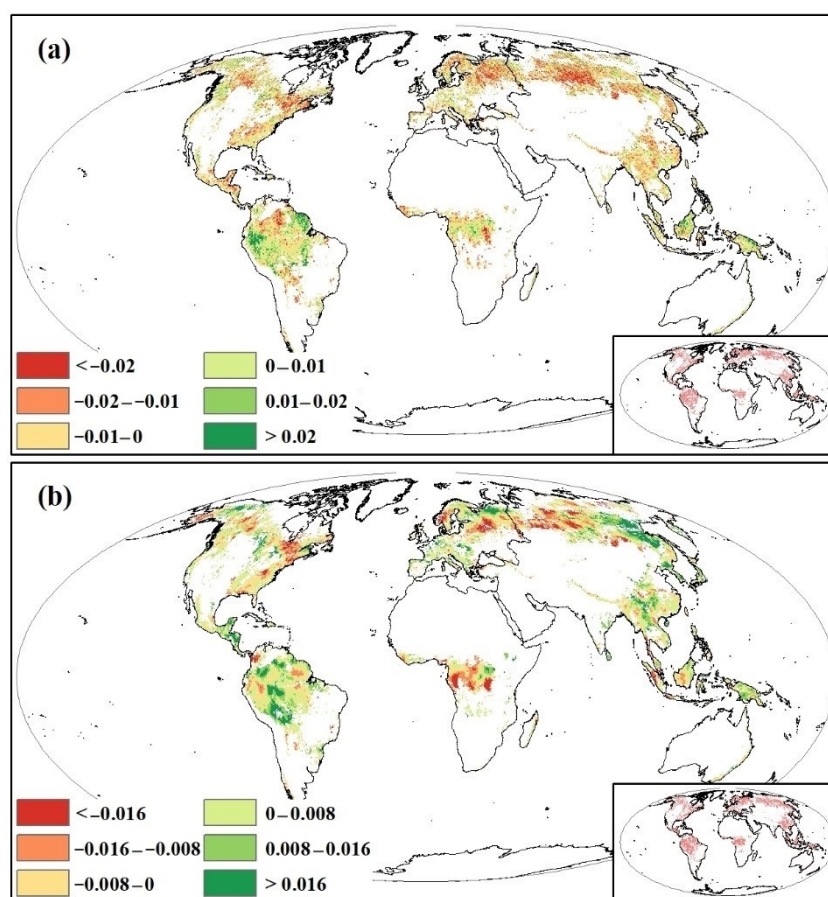


**Figure 2.** The trend of moving window in partial correlation between LAI (a), ET (b), and VPD across the global forest ecosystem in spatial pattern. The inset maps in lower right represent the significance at the level of 0.05.

The temporal trend of the growing season SPEI and SWC are shown in Figure 3. In general, the SPEI and SWC appeared as predominantly positive and negative trends, respectively, with the former accounting for 63.2% (9.3% of the pixels were significant) and the latter for 56.4% (23.4% of the pixels were significant). The pixels with increased SPEI values were concentrated in eastern North America, the Siberian plains of western Russia, and western South Africa, while the decreasing pixels were located in the plains of Eastern Europe, southern Siberia, the subtropical regions of China, and the central regions of South America (Figure 3a). As for the SWC (Figure 3b), the areas with increasing pixel values were mainly in North America and parts of Russia, while other areas such as the plains of Eastern Europe, southern Siberia, and central Africa were where the SWC decreases.

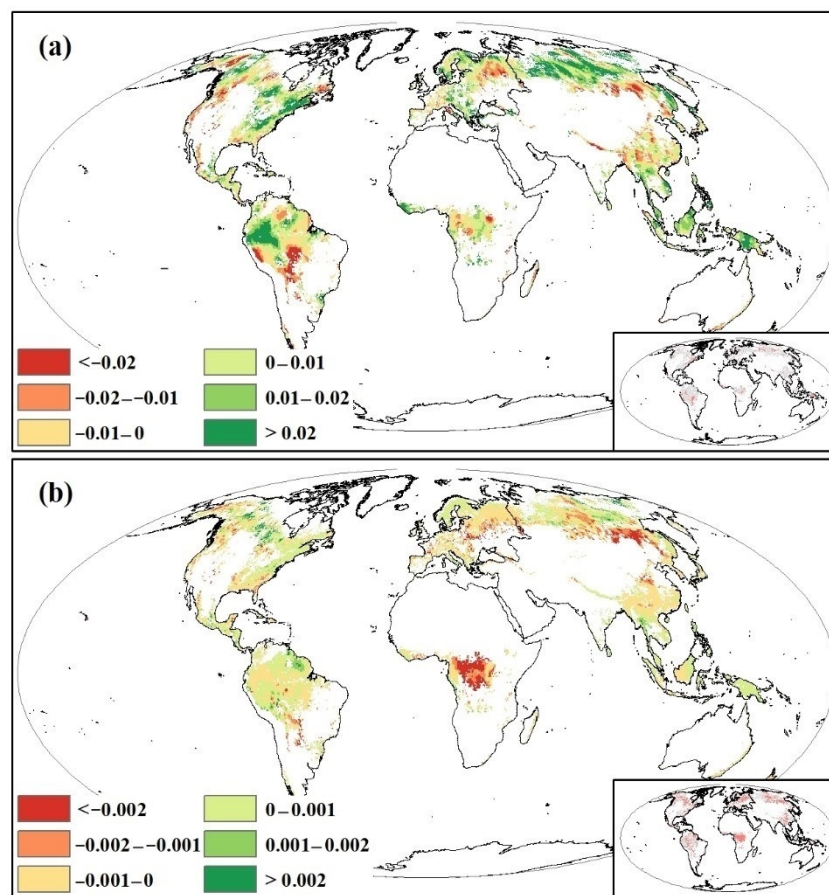


**Figure 3.** The spatial patterns of temporal trend for SPEI (a) and SWC (b) across the global forest ecosystem. The insets map in lower right represents the significance at the level of 0.05.

To further clarify the relationship between the LAI, ET, and SWC, we performed the correlation analysis based on the ten-year moving window averages. As a whole, the positive correlation pixels for the LAI and SWC (Figure 4a) accounted for 53.8% (29.5% of the pixels were significant), mainly distributed in the plains of Eastern Europe, southern Siberia, the subtropics of China, and parts of the Amazon. In comparison, the negatively correlated pixels mainly occurred in the Siberian plains of western Russia, western North America, central Africa, and parts of South America. The proportion of significantly negatively correlated pixels was relatively small, only occupying 23.6% of the study area. We also observed that about 50.1% (27.5% of the pixels were significant) of the pixels displayed a positive correlation between the ET and SWC (Figure 4b), most of them distributed in the plains of Eastern Europe, eastern Russia, central Africa, and parts of the Amazon. For those negatively correlated pixels, they were mainly located in the Siberian Plain in western Russia, eastern and southwestern China, and parts of the Amazon.

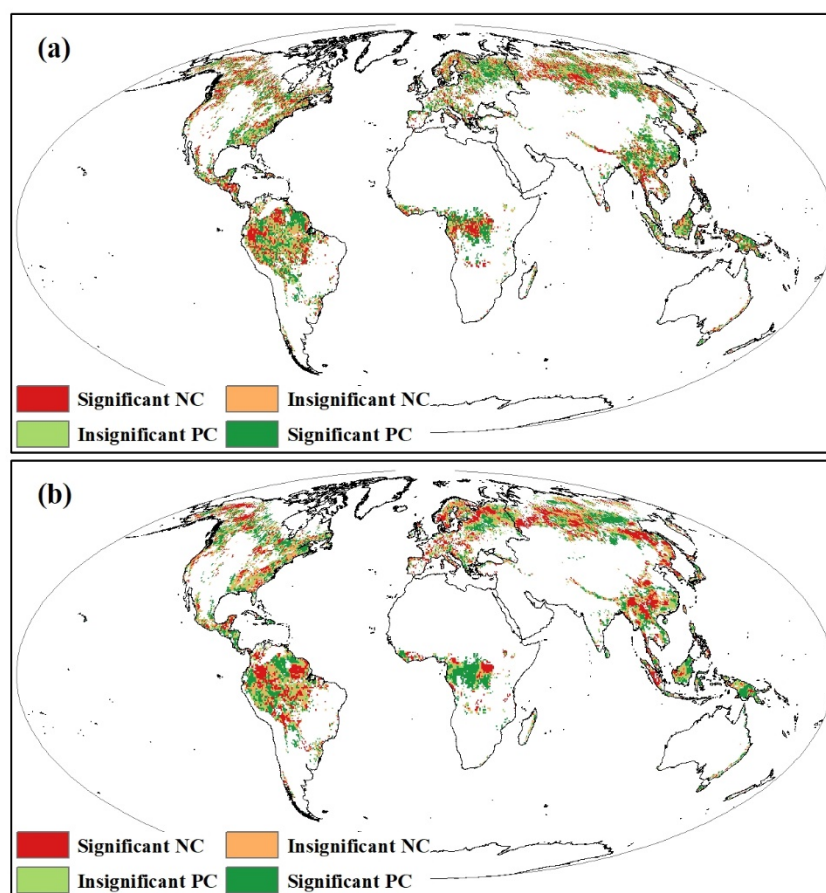


**Figure 4.** The spatial patterns of correlation between the effects of LAI (a), ET (b), and SWC based on ten-year moving window average across the global forest ecosystem. Note: NC and PC represent negative correlation and positive correlation, respectively.

#### 4. Discussion

Overall, the response of the forest LAI and ET to the VPD varied with the spatial water gradients. The VPD may also indicate atmospheric dryness. Increased atmospheric water demand caused by an increasing VPD reduces plant photosynthesis and transpiration by controlling the stomatal activity and xylem conductance [14,30]. A typical plant response to an increasing VPD is to close the stomata to minimize the water loss and avoid excessive water tension in the xylem at the expense of reducing or stopping photosynthesis [5,31]. This negative response of plant photosynthesis and transpiration to an increasing VPD has always been observed in water-limited regions [4,5]. This is because, in these regions, xeric species tend to adopt a more conservative sequence to prevent severe tissue damage through tighter stomatal regulation and higher resistance to embolism [32]. In contrast, the LAI and ET can resist the atmospheric dryness caused by an increasing VPD across the mostly forest regions, especially for the water-rich regions. Most forests are distributed in water-rich regions. Although annual precipitation in most boreal forest regions is always less than 500 mm, they are not water-limited due to the high soil water-holding capacity of high soil organic matter [33] and low water loss under thermal constraint. Mesic species adopt a riskier sequence through looser stomatal regulation to maximize carbon uptake at the expense of hydraulic safety [32]. Plant root systems could partly determine how a certain soil water availability is translated into leaf water potential, which is strongly correlated with stomatal activity [34]. Forests can extract deeper soil water through vigorous root systems and allow them to maintain higher leaf water potential and stomatal openness under dryness stress (such as under a VPD) [7,19]. In addition, the subtropical and tropical forests always have light limitations and thus plants could tend to maintain their stomata

openness at the cost of water loss in response to an increasing VPD [7,35]. Furthermore, new leaves have a higher photosynthetic capacity than the leaves they replaced in the dry season, compensating for the negative stomatal response to increased dryness [15]. In line with our study, a recent global study also has shown that the VPD has weakly negative or even positive impacts on vegetation productivity in most of boreal southern China, India, and tropical rainforests [16].

In contrast, there is a significant negative response of ET and the LAI to the VPD in the seasonally dry regions of forests. Although these forest regions are always classified as water-rich regions, the seasonal dryness could lead to the negative response of the LAI and ET to the VPD. The majority of seasonally dry ecosystems become more isohydric during the sunnier and drier seasons, as they are most at risk of hydraulic failure [18,19]. Like other forests in the water-rich regions, forests could also utilize soil water via deep roots to resist the atmospheric water deficits [36], but forests may restrain stomatal activity to avoid hydraulic failure as the SWC continues to decrease during the dry seasons [7]. Similar to seasonal drought regions, tropical forests also experience seasonal dryness, whereas their co-variation patterns are different. Except for the plant water use strategy and soil water conditions, these differences could also be attributed to plant phenology developments. Certainly, we expect that future research combining multiple factors (water use strategy, phenology developments, water availability, etc.) is urgently needed to help shed light on these differences.

Climate scenarios and our observations present an enhancement of the water deficit and heatwaves over the past few decades in Eastern Europe [37,38]. In particular, frequent heatwaves, evidenced by marked decreases in the ESI, co-occur with high temperatures and low SWC, amplifying the negative impacts of a VPD on vegetation growth and ET by pushing atmospheric dryness up to the peak [8,39]. Thus, the negative response of the LAI and ET is exacerbated by a drop in the water supply in Eastern Europe on a temporal scale.

With an improving water supply, the positive regulatory effects disappeared in the moisture-rich regions of Central Siberia, suggesting that the positive co-variation was withering on a temporal scale. This is in reasonable agreement with recent work in humid regions, where the positive sensitivity of the vegetation growth to the VPD in wet gradients is less than in other gradients [7,40]. Given the increasing likelihood for wet and cloudy conditions to coincide over the past 30 years, as evidenced by decreases in SR, the decreases seem not to be responsible for the VPD because an adequate water supply makes it less possible for atmospheric dryness to occur. It is possible that a water surplus can limit vegetation growth due to waterlogging or the fact that temperatures and solar radiation limit productivity or ET in some wetter years [40,41].

In this study, we mainly used the remote sensing datasets combined with a statistical correlation analysis to analyze the response of the LAI and ET to the VPD. This may increase uncertainties in the VPD impacts. Many indicators (e.g., leaf hydraulic traits) related to the plants' water use strategy were not measured in this study, which may influence the ecological response mechanisms of the VPD effects [17,42]. In view of the above, future field experiments on extreme drought should comprehensively measure indicators of the plant water use strategy. In addition, we expect future earth system models to fully consider the effects of the VPD on the forest ecosystem structure and functions.

## 5. Conclusions

This study utilized long-term remote sensing data to evaluate the response of the LAI and ET to the VPD via multiple statistical analyses across the global forest ecosystem. The results showed that negative partial correlations were found in over 50% of the regions between the LAI, ET, and VPD, indicating the suppression effect of vegetation growth by the VPD. Moreover, this suppression effect is getting stronger, especially in the plains of Eastern Europe and the Siberian Plain of western Russia. We also observed a decreasing trend for both the SPEI and SWC in the plains of Eastern Europe, which shows the region is becoming increasingly drier. Furthermore, the regions of the LAI and ET in the above area

exhibited a significant positive correlation with the SWC based on the moving window average. This study would deepen our understanding of vegetation and ET responses to an increased atmospheric VPD across the global forest in the context of climate change. Our research potentially improves our knowledge and understanding of the negative impacts of the VPD on forests and the predictions of forest ecosystem functioning and bio-diversity in response to climate change.

**Author Contributions:** Conceptualization, R.W., M.Q., P.J. and B.S.; methodology, P.J. and R.W.; software, R.W. and M.Q.; data curation, M.Z. and Y.T.; writing—original draft preparation, R.W. and M.Q., writing—review and editing, P.J., B.S., F.Y., B.L., M.Z., Y.F. and Y.T.; visualization, F.Y., M.Q. and B.L.; supervision, P.J. and B.S. All authors have read and agreed to the published version of the manuscript.

**Funding:** This work was supported by the National Key R&D Program of China (Grant No. 2022YFF0801301), the Key Project of Liaoning Provincial Meteorological Bureau (Grant No. LNCP202205), the Annual Fund Project of Liaoning Provincial Meteorological Bureau for 2024, and the Key Laboratory Project of Agricultural Meteorological Disasters in Liaoning Province in 2023 (Grant No. 2023SYIAEKFMS30).

**Institutional Review Board Statement:** Not applicable.

**Informed Consent Statement:** Not applicable.

**Data Availability Statement:** The codes used in this study are available upon request from the authors. The data are not publicly available due to privacy.

**Acknowledgments:** We acknowledge the support of all co-authors for their constructive and helpful comments and the organization of this study.

**Conflicts of Interest:** The authors declare that this research was conducted in the absence of any commercial or financial relationships that could be construed as potential conflicts of interest.

## References

1. Le Quéré, C.; Andrew, R.M.; Friedlingstein, P.; Sitch, S.; Pongratz, J.; Manning, A.C.; Korsbakken, J.I.; Peters, G.P.; Canadell, J.G.; Jackson, R.B.; et al. Global carbon budget 2017. *Earth Syst. Sci. Data* **2018**, *10*, 405–448. [[CrossRef](#)]
2. Pan, Y.; Birdsey, R.A.; Fang, J.; Houghton, R.; Kauppi, P.E.; Kurz, W.A.; Phillips, O.L.; Shvidenko, A.; Lewis, S.L.; Canadell, J.G.; et al. A large and persistent carbon sink in the world's forests. *Science* **2011**, *333*, 988–993. [[CrossRef](#)]
3. Pugh, T.A.M.; Lindeskog, M.; Smith, B.; Poulter, B.; Arneeth, A.; Haverd, V.; Calle, L. Role of forest regrowth in global carbon sink dynamics. *Proc. Natl. Acad. Sci. USA* **2019**, *116*, 4382–4387. [[CrossRef](#)]
4. Yuan, W.; Zheng, Y.; Piao, S.; Ciais, P.; Lombardozzi, D.; Wang, Y.; Ryu, Y.; Chen, G.; Dong, W.; Hu, Z.; et al. Increased atmospheric vapor pressure deficit reduces global vegetation growth. *Sci. Adv.* **2019**, *5*, eaax1396. [[CrossRef](#)]
5. Sulman, B.N.; Roman, D.T.; Yi, K.; Wang, L.; Phillips, R.P.; Novick, K.A. High atmospheric demand for water can limit forest carbon uptake and transpiration as severely as dry soil. *Geophys. Res. Lett.* **2016**, *43*, 9686–9695. [[CrossRef](#)]
6. Ding, J.; Yang, T.; Zhao, Y.; Liu, D.; Wang, X.; Yao, Y.; Peng, S.; Wang, T.; Piao, S. Increasingly important role of atmospheric aridity on Tibetan alpine grasslands. *Geophys. Res. Lett.* **2018**, *45*, 2852–2859. [[CrossRef](#)]
7. Chen, N.; Song, C.; Xu, X.; Wang, X.; Cong, N.; Jiang, P.; Zu, J.; Sun, L.; Song, Y.; Zuo, Y.; et al. Divergent impacts of atmospheric water demand on gross primary productivity in three typical ecosystems in China. *Agric. For. Meteorol.* **2021**, *307*, 108527. [[CrossRef](#)]
8. Fu, Z.; Ciais, P.; Prentice, I.C.; Gentine, P.; Makowski, D.; Bastos, A.; Luo, X.; Green, J.K.; Stoy, P.C.; Yang, H.; et al. Atmospheric dryness reduces photosynthesis along a large range of soil water deficits. *Nat. Commun.* **2022**, *13*, 989. [[CrossRef](#)] [[PubMed](#)]
9. Liu, L.; Gudmundsson, L.; Hauser, M.; Qin, D.; Li, S.; Seneviratne, S.I. Soil moisture dominates dryness stress on ecosystem production globally. *Nat. Commun.* **2020**, *11*, 4892. [[CrossRef](#)]
10. Green, J.K.; Seneviratne, S.I.; Berg, A.M.; Findell, K.L.; Hagemann, S.; Lawrence, D.M.; Gentine, P. Large influence of soil moisture on long-term terrestrial carbon uptake. *Nature* **2019**, *565*, 476–479. [[CrossRef](#)]
11. He, B.; Chen, C.; Lin, S.; Yuan, W.; Chen, H.W.; Chen, D.; Zhang, Y.; Guo, L.; Zhao, X.; Liu, X. Worldwide impacts of atmospheric vapor pressure deficit on the interannual variability of terrestrial carbon sinks. *Natl. Sci. Rev.* **2022**, *9*, nwab150. [[CrossRef](#)] [[PubMed](#)]
12. Williams, A.P.; Allen, C.D.; Macalady, A.K.; Griffin, D.; Woodhouse, C.A.; Meko, D.M.; Swetnam, T.W.; Rauscher, S.A.; Seager, R.; Grissinomayer, H.D. Temperature as a potent driver of regional forest drought stress and tree mortality. *Nat. Clim. Chang.* **2013**, *3*, 292–297. [[CrossRef](#)]

13. Seager, R.; Hooks, A.; Williams, A.P.; Cook, B.; Nakamura, J.; Henderson, N. Climatology, variability, and trends in the US vapor pressure deficit, an important fire-related meteorological quantity. *J. Appl. Meteorol. Climatol.* **2015**, *54*, 1121–1141. [[CrossRef](#)]
14. Novick, K.A.; Ficklin, D.L.; Stoy, P.C.; Williams, C.A.; Bohrer, G.; Oishi, A.C.; Papuga, S.A.; Blanken, P.D.; Noormets, A.; Sulman, B.N.; et al. The increasing importance of atmospheric demand for ecosystem water and carbon fluxes. *Nat. Clim. Chang.* **2016**, *6*, 1023–1027. [[CrossRef](#)]
15. Green, J.; Berry, J.; Ciais, P.; Zhang, Y.; Gentile, P. Amazon rainforest photosynthesis increases in response to atmospheric dryness. *Sci. Adv.* **2020**, *6*, eabb7232. [[CrossRef](#)]
16. Song, Y.; Jiao, W.; Wang, J.; Wang, L. Increased Global Vegetation Productivity Despite Rising Atmospheric Dryness over the Last Two Decades. *Earth's Future* **2022**, *10*, e2021EF002634. [[CrossRef](#)]
17. Rogiers, S.Y.; Greer, D.H.; Hatfield, J.M.; Hutton, R.J.; Clarke, S.J.; Hutchinson, P.A.; Somers, A. Stomatal response of an anisohydric grapevine cultivar to evaporative demand, available soil moisture and abscisic acid. *Tree Physiol.* **2012**, *32*, 249–261. [[CrossRef](#)]
18. Konings, A.G.; Gentile, P. Global variations in ecosystem-scale isohydricity. *Glob. Chang. Biol.* **2017**, *23*, 891–905. [[CrossRef](#)]
19. Jiang, P.; Meinzer, F.C.; Wang, H.; Kou, L.; Dai, X.; Fu, X. Belowground determinants and ecological implications of shrub species' degree of isohydry in subtropical pine plantations. *New Phytol.* **2020**, *226*, 1656–1666. [[CrossRef](#)]
20. Stevenson, S.; Coats, S.; Touma, D.; Cole, J.; Lehner, F.; Fasullo, J.; Otto-Bliesner, B. Twenty-first century hydroclimate: A continually changing baseline, with more frequent extremes. *Proc. Natl. Acad. Sci. USA* **2022**, *119*, e2108124119. [[CrossRef](#)]
21. Xiao, Z.; Liang, S.; Wang, J.D.; Chen, P.; Yin, X.J.; Zhang, L.Q.; Song, J.L. Use of general regression neural networks for generating the GLASS leaf area index product from time-series MODIS surface reflectance. *IEEE Trans. Geosci. Remote Sens.* **2014**, *52*, 209–223. [[CrossRef](#)]
22. Liang, S.; Cheng, J.; Jia, K.; Jiang, B.; Liu, Q.; Xiao, Z.; Yao, Y.; Yuan, W.; Zhang, X.; Zhao, X.; et al. The Global Land Surface Satellite (GLASS) Product Suite. *Bull. Am. Meteorol. Soc.* **2021**, *102*, E323–E337. [[CrossRef](#)]
23. Li, X.; Qu, Y. Evaluation of Vegetation Responses to Climatic Factors and Global Vegetation Trends using GLASS LAI from 1982 to 2010. *Can. J. Remote Sens.* **2019**, *44*, 357–372. [[CrossRef](#)]
24. Bai, Y.; Li, S.; Liu, M.; Guo, Q. Assessment of vegetation change on the Mongolian Plateau over three decades using different remote sensing products. *J. Environ. Manag.* **2022**, *317*, 115509. [[CrossRef](#)]
25. Martens, B.; Miralles, D.G.; Lievens, H.; van der Schalie, R.; de Jeu, R.A.M.; Fernández-Prieto, D.; Beck, H.E.; Dorigo, W.A.; Verhoest, N.E.C. GLEAM v3: Satellite-based land evaporation and root-zone soil moisture. *Geosci. Model Dev.* **2017**, *10*, 1903–1925. [[CrossRef](#)]
26. Beguería, S.; Vicente-Serrano, S.M.; Angulo-Martínez, M. A Multiscalar Global Drought Dataset: The SPEIbase: A New Gridded Product for the Analysis of Drought Variability and Impacts. *Bull. Am. Meteorol. Soc.* **2010**, *91*, 1351–1356. [[CrossRef](#)]
27. Vicente-Serrano, S.M.; Beguería, S.; López-Moreno, J.I.; Angulo, M.; El Kenawy, A. A New Global 0.5° Gridded Dataset (1901–2006) of a Multiscalar Drought Index: Comparison with Current Drought Index Datasets Based on the Palmer Drought Severity Index. *J. Hydrometeorol.* **2010**, *11*, 1033–1043. [[CrossRef](#)]
28. Piao, S.; Nan, H.; Huntingford, C.; Ciais, P.; Friedlingstein, P.; Sitch, S.; Peng, S.; Ahlstrom, A.; Canadell, J.G.; Cong, N.; et al. Evidence for a weakening relationship between interannual temperature variability and northern vegetation activity. *Nat. Commun.* **2014**, *5*, 5018. [[CrossRef](#)]
29. Zu, J.; Zhang, Y.; Huang, K.; Liu, Y.; Chen, N.; Cong, N. Biological and climate factors co-regulated spatial-temporal dynamics of vegetation autumn phenology on the Tibetan Plateau. *Int. J. Appl. Earth Obs. Geoinf.* **2018**, *69*, 198–205. [[CrossRef](#)]
30. Grossiord, C.; Buckley, T.N.; Cernusak, L.A.; Novick, K.A.; Poulter, B.; Siegwolf, R.T.W.; Sperry, J.S.; McDowell, N.G. Plant responses to rising vapor pressure deficit. *New Phytol.* **2020**, *226*, 1550–1566. [[CrossRef](#)] [[PubMed](#)]
31. Running, S.W. Environmental control of leaf water conductance in conifers. *Can. J. For. Res.* **1976**, *6*, 104–112. [[CrossRef](#)]
32. Jin, Y.; Hao, G.; Hammond, W.M.; Yu, K.; Liu, X.; Ye, Q.; Zhou, Z.; Wang, C. Aridity-dependent sequence of water potentials for stomatal closure and hydraulic dysfunctions in woody plants. *Glob. Chang. Biol.* **2023**, *29*, 2030–2040. [[CrossRef](#)] [[PubMed](#)]
33. Stack, S.; Jones, C.; Bockstette, J.; Jacobs, D.F.; Landhäusser, S.M.J.E.E. Surface and subsurface material selections influence the early outcomes of boreal upland forest restoration. *Ecol. Eng.* **2020**, *144*, 105705. [[CrossRef](#)]
34. Meinzer, F.C.; Woodruff, D.R.; Marias, D.E.; Smith, D.D.; McCulloh, K.A.; Howard, A.R.; Magedman, A.L. Mapping 'hydroscales' along the iso- to anisohydric continuum of stomatal regulation of plant water status. *Ecol. Lett.* **2016**, *19*, 1343–1352. [[CrossRef](#)] [[PubMed](#)]
35. Yu, G.; Zhang, L.; Sun, X.; Fu, Y.; Wen, X.; Wang, Q.; Li, S.; Ren, C.; Song, X.; Liu, Y. Environmental controls over carbon exchange of three forest ecosystems in eastern China. *Glob. Chang. Biol.* **2008**, *14*, 2555–2571. [[CrossRef](#)]
36. Jiang, P.; Wang, H.; Meinzer, F.C.; Kou, L.; Dai, X.; Fu, X. Linking reliance on deep soil water to resource economy strategies and abundance among coexisting understorey shrub species in subtropical pine plantations. *New Phytol.* **2020**, *225*, 222–233. [[CrossRef](#)]
37. Seneviratne, S.I.; Corti, T.; Davin, E.L.; Hirschi, M.; Jaeger, E.B.; Lehner, I.; Orlowsky, B.; Teuling, A.J. Investigating soil moisture–climate interactions in a changing climate: A review. *Earth-Sci. Rev.* **2010**, *99*, 125–161. [[CrossRef](#)]
38. Liu, X.; He, B.; Guo, L.; Huang, L.; Yuan, W.; Chen, X.; Hao, X.; Xie, X.; Zhang, Y.; Zhong, Z.; et al. European Carbon Uptake has Not Benefited from Vegetation Greening. *Geophys. Res. Lett.* **2021**, *48*, e2021GL094870. [[CrossRef](#)]

39. Wang, S.; Zhang, Y.; Ju, W.; Porcar-Castell, A.; Ye, S.; Zhang, Z.; Brümmer, C.; Urbaniak, M.; Mammarella, I.; Juszczak, R.; et al. Warmer spring alleviated the impacts of 2018 European summer heatwave and drought on vegetation photosynthesis. *Agric. For. Meteorol.* **2020**, *295*, 108195. [[CrossRef](#)]
40. Rigden, A.J.; Mueller, N.D.; Holbrook, N.M.; Pillai, N.; Huybers, P. Combined influence of soil moisture and atmospheric evaporative demand is important for accurately predicting US maize yields. *Nat. Food* **2020**, *1*, 127–133. [[CrossRef](#)]
41. Jiao, W.; Wang, L.; Smith, W.K.; Chang, Q.; Wang, H.; D’Odorico, P. Observed increasing water constraint on vegetation growth over the last three decades. *Nat. Commun.* **2021**, *12*, 3777. [[CrossRef](#)] [[PubMed](#)]
42. Novick, K.A.; Konings, A.G.; Gentile, P. Beyond soil water potential: An expanded view on isohydricity including land–atmosphere interactions and phenology. *Plant Cell Environ.* **2019**, *42*, 1802–1815. [[CrossRef](#)] [[PubMed](#)]

**Disclaimer/Publisher’s Note:** The statements, opinions and data contained in all publications are solely those of the individual author(s) and contributor(s) and not of MDPI and/or the editor(s). MDPI and/or the editor(s) disclaim responsibility for any injury to people or property resulting from any ideas, methods, instructions or products referred to in the content.